Riom, Wilhem; Shettigar, Nithin Achutha; Toorman, Erik A.

Process based model for riverine plastic fluxes

Process based model for riverine plastic fluxes

Wilhem Riom[1], Nithin Achutha Shettigar[1], Erik Toorman[1]
wilhem.riom@kuleuven.be, Leuven, Belgium
[1] Hydraulics Laboratory, Department of Civil Engineering, KU
Leuven, Kasteelpark Arenberg 40, Box 2448, 3001 Leuven, Belgium

Abstract - **Plastic pollution in the sea and oceans is an increasing concern, especially when considering its impact on the biome, biota and eventual hazardous consequences on human activities and health. Rivers are the major pathways for plastic and microplastics (MP, size <5mm) exportation toward the ocean. Adopting modelling approaches may increase our understanding of this pathway as well as the distribution and fate of MPs in the environment. Eulerian approaches permit to account for plastic concentration, number of particles or mass, temporal and spatial evolution and is appropriate for smaller particles. A coupled TELEMAC-2D+GAIA only allows to model settling particles as sediments preventing to account for the full range of plastic particles behaviour (buoyant and settling). The LABPLAS (Land-Based Solutions for Plastics in the Sea) project aims at developing a three-layered model representing microplastics dispersal and interaction with their environment over riverine and coastal areas. In this model MPs are modelled as tracers transported at three levels: at the surface, in suspension and as bedload. Material exchanges between floating and suspended layers are possible through a buoyant and a mixing flux. This three-layered module was developed based on the existing TELEMAC-2D+GAIA code and results in mass-conservative and coherent results when applied to simple flumes with and without flow. However, the presented implementation induces non negligeable mass creation (or losses) when the domain includes inter tidal areas. The full schematised module is visible in Figure 1.**

Keywords: pollution, microplastics, freshwater, coastal water, tracers, TELEMAC-2D, GAIA.

I. INTRODUCTION

The, largely acknowledged, extent of plastic pollution in the marine environment [1] has for main origin, land-based sources with debris mostly being conveyed by freshwater discharges [2]. Understanding rivers pollution levels and export mechanisms is thereby, crucial to capture the full scope of plastic waste at sea [3]. Within the LABPLAS project, a process-based model for riverine plastic fluxes is under development. This model must faithfully represent both horizontal transport and the complex vertical settling of plastics. Indeed, the plastic waste shows large polydispersity in term of shape, size, density and thus buoyancy is the main driver governing the vertical dispersion (suspension in the water column, settling towards the bottom or buoyancy at the surface) of plastic particles both at sea [4] [5] and in freshwater [6]. Complementary mechanisms such as biofouling [7], weathering [8], mechanical stresses [9] and interactions with sediments flocs [10] may alter plastic particle and hence their fate in waterways. These mechanisms altogether, may explain why normally buoyant plastics (PE and PP) were found at the bottom of the Elbe River during a sampling campaign [11]. Based on the TELEMAC system, and specifically TELEMAC-2D and GAIA, for coupled depth averaged flows with sediment transports, this paper presents the theorization and validation of a three-layer model allowing the transport of microplastics over three layers: at the surface, in suspension and in the bedload.

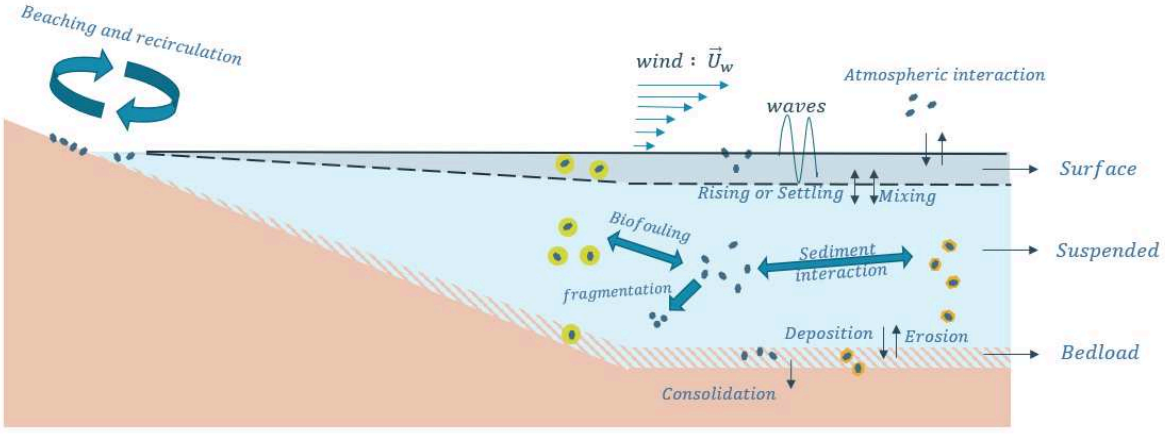

Figure 12. Schematic representation of the three-layered model

II. THEORY AND MODEL IMPLEMENTATION

A. Model description

The proposed three-layer model has been developed according to how TELEMAC-2D and GAIA are already coupled for sediments transport. A class of sediment can evolve in suspension and/or in one or several bed layers. Here, a class of plastic can be transported in suspension, in the bedload and at the surface of the water.

This section describes the theory behind the horizontal transport equation in the water column (suspension and surface) and the vertical transfer of mass. The horizontal bedload transport and vertical exchanges between suspension and the bedload is kept as already implemented in GAIA [12]. Plastic classes will be designated by the term tracer as the following theory is not limited to plastic particles only.

Considering a fluid of viscosity ν_{ts} in a shallow water flow, solved by TELEMAC-2D. The free surface elevation is $h = h(x, y, t)$, and the depth-averaged velocity field is $\boldsymbol{u_s}$=$(u_s, v_s)(x, y, t)$, with, x, y and t respectively the space and time variables. Suspended tracers transport follows the 2D advection-diffusion equation (1).

$$\frac{\partial hC_s}{\partial t} + \frac{\partial hu_s C_s}{\partial x} + \frac{\partial hv_s C_s}{\partial y} = \frac{\partial}{\partial x}\left(h\frac{\nu_{ts}}{S_c}\frac{\partial C_s}{\partial x}\right) + \frac{\partial}{\partial y}\left(h\frac{\nu_{ts}}{S_c}\frac{\partial C_s}{\partial y}\right) + M + B + E - D \quad (1)$$

with $S_c = 0.7$ the turbulent Schmidt number developed in [13] and [14], E and D, are respectively the erosion and deposition fluxes between the suspended layer and the bed which are handled by Gaia [15]. M and B are the mixing and buoyant fluxes between the suspended and surface layer. They are introduced next.

A surface layer, of zero thickness, is introduced and characterized by a fluid viscosity, ν_{tf}, and a surface velocity field $\boldsymbol{u_f} = (u_f, v_f)(x, y, t)$ function of the shallow-water velocity $\boldsymbol{u_s}$ and of a given vertical velocity profile (e.g. constant, linear, logarithmic, power-law). In this study, for simplification purposes, the profile is considered constant. This surface layer can transport tracers of concentration, $C_f(x, y, t)$, following the advection-diffusion equation under its non-conservative form (2):

$$\frac{\partial C_f}{\partial t} + \frac{\partial u_f C_f}{\partial x} + \frac{\partial v_{tf} C_f}{\partial y} = \frac{\partial}{\partial x}\left(\frac{\nu_{tf}}{S_c}\frac{\partial C_f}{\partial x}\right) + \frac{\partial}{\partial y}\left(\frac{\nu_{tf}}{S_c}\frac{\partial C_f}{\partial y}\right) - \frac{(M + B)}{h} \quad (2)$$

where the mixing, M and buoyancy, B allow coupling between (1) and (2) through vertical mass transfer between the surface and the suspension layer. The fluxes exist for buoyant and settling classes of tracers. B represents the vertical movement of particles due to their buoyancy. It is defined here following the Partheniades approach. Equations (3) and (4) present respectively this flux for a settling tracer, of positive settling velocity $w_s > 0$, and for a buoyant tracer class ($w_s < 0$).

$$B = p_f w_s C_f \quad (3)$$

$$B = -p_s w_s C_s \quad (4)$$

where p_f and p_s are probability function taken equal to the unit h. If the tracer class is buoyant, B will add mass in the surface layer while removing mass from the suspended layer.

Usually, the mixing flux, M, counterbalance the rising or settling and allows equilibrium of the vertical concentration distribution. Mixing is important in affecting the vertical distribution of plastic in water [9] [5]. Indeed, vertical turbulent mixing dampens the buoyant vertical transfer. Equation (5) shows it usual definition with a continuous concentration, C, and viscosity, ν_t, over the vertical axis z.

$$M = \frac{\nu_t}{S_c}\frac{\partial C}{\partial z} \quad (5)$$

However, to match our three-layered model, one can approximate the vertical derivative by its first order as in (6):

$$M = \frac{\nu_{tf}}{S_c}\frac{C_f - C_s}{h} \quad (6)$$

We choose here the viscosity at the surface and the free surface elevation, h as characteristic distance for the derivative. In (2), and (6), h is chosen as characteristic height for the mass transfer, another distance may be a lead for improvement. Using an exponential vertical profile for the buoyant plastic concentration could be directly inspired from [10]. Using a Rouse profile may be directly applicable to settling plastic classes. In equation (1), the erosion and deposition fluxes are only defined if the tracer is settling. Hence, buoyant plastics are assumed to never reach the bottom without considering other factors (e.g. biofouling, sediments interaction) that will change their settling.

As the surface layer is assumed to have no thickness, the surface tracers concentration dimension is a surface mass ($[M][L]^{-2}$). This causes dimensional issues with the presented definition of the equations. This will be dealt with directly in the implementation section.

B. Implementation

1) New variables

The way that the surface layer was added into the TELEMAC-2D code is first, by declaring the following sets of variables:

- The surface velocity field called U_SURF, V_SURF and a new surface viscosity field named VISCT_SURF. These variables are identical in format and shape to their existing counterpart.

- A set of tracers for the surface concentrations: one for the previous calculation step TN_SURF and one for the current one: T_SURF. These tracers are created identical in size to TN and T which become here the suspended tracer concentration. This allows to conserve the coupling between suspended concentration, dealt with in TELEMAC-2D, and bedload mass, solved by GAIA.
- The settling velocity although considered here constant in space, was adapted in format to allow spatial variations. This will become useful at later stage of the module development where local variation of the settling velocity may occur due to spatial biological variations.
- Variables related to the boundary conditions of the suspended tracers were also duplicated and named just by juxtaposing the suffix "_SURF" after their name.
- TEXP_SURF, TIMP_SURF, TSCEXP_SURF respectively the explicit, implicit and punctual source of mass for the surface layer were implemented as clones of TEXP, TIMP and TSCEXP.

The interesting modified or added variables are autonomously exited in the resulting selafin file: if n tracers are followed through a simulation, then the output selafin file will have n+2 new fields: VELOCITY SURF U, VELOCITY SURF V, T_SURF 1, T_SURF 2, …, T_SURF N.

2) Algorithmic resolution

This section focuses on the numerical solution of the quantities introduced in the module. It is supposed that all the quantities at timestep N are known. Table I shows the order of the calculation to derive the quantities at time $N+1$. No changes were done to how Telemac2D and Gaia are coupled. From this table, the coupling is assured by steps 3 and 5. However, this coupling must assure adequation between the dimensions of the numerical counterpart of equations (1) and (2).

3) Vertical fluxes implementation

The buoyant flux is added in the numerical counterpart of equations (1) and (2) either implicitly or explicitly depending on the buoyancy of the tracer class and the concerned layer. The implementation is summarized in Table II. Where SM, SMH and SMI are respectively the explicit non conservative, conservative and implicit source or sink terms added in the numerical advection-diffusion equations. SM and SMH are added as such while for SMI and a tracer F, the added term is $\frac{SMI\ F}{H}$, with H, the numerical variable designating the free surface elevation. To ease the numerical implementation, the mixing flux is divided in two fluxes: one depends on the suspended concentration while the other depends on the surface concentration (see (7)). For a given layer, this flux is now made of two independent terms. Table III shows the implementation method of these terms into the numerical equations.

$$M = \frac{\nu_{tf}}{S_c}\frac{C_f - C_s}{h} = \frac{\nu_{tf}}{S_c}\frac{C_f}{h} - \frac{\nu_{tf}}{S_c}\frac{C_s}{h} \qquad (7)$$

ν_t is the turbulent viscosity of the interface, taken equal to its value in the surface layer.

Table I Module order of resolution

Step	***Resolution***	*Derived variable*
1.	Solve the Saint-Venant Equation.	U^{N+1}, V^{N+1}, H^{N+1}
2.	Derive the surface velocity and the surface turbulent viscosity.	U_SURF^{N+1}, V_SURF^{N+1}, $HUCT\_SURF^{N+1}$
3.	Calculate the fluxes from bedload to suspension and surface to suspension.	$TEXP, TIMP, TSCEXP$
4.	*Solve the advection-diffusion of the suspended concentration*	C_s^{N+1}
5.	*Calculate the fluxes from suspension to surface.*	$TEXP\_SURF$, $TIMP\_SURF$, $TSCEXP\_SURF$
6.	*Solve the advection diffusion of the surface layer*	C_f^{N+1}
7.	*Calculate the fluxes from suspension to bedload*	*GAIA*
8.	Solve bedload transport.	

Table II Buoyant flux numerical implementation

Buoyancy/Layer	**Suspended** step 3.	**Surface** step 5.
Settling $w_s > 0$	$\boldsymbol{SMH} = +\frac{p_s w_s C_f^{N+1}}{h^2}$	$\boldsymbol{SMI} = -p_f w_s$
Buoyant $w_s < 0$	$\boldsymbol{SMI} = -p_s w_s$	$\boldsymbol{SM} = -p_s w_s C_s^{N+1}$

Table III Mixing flux numerical implementation

Layer	$\frac{\boldsymbol{\nu_{tf}}}{\boldsymbol{S_c}}\frac{\boldsymbol{C_s}}{\boldsymbol{h}}$	**Flux**	$\frac{\boldsymbol{\nu_{tf}}}{\boldsymbol{S_c}}\frac{\boldsymbol{C_f}}{\boldsymbol{h}}$	**Flux**
Suspended step 3.	*Sink*	$\boldsymbol{SMI} = -\frac{\upsilon_t}{Sc}$	*Source*	$\boldsymbol{SMH} = +\frac{\upsilon_t}{Sc}\frac{C_f^{N+1}}{h^2}$
Surface step 5.	*Source*	$\boldsymbol{SM} = +\frac{\upsilon_t}{Sc}\frac{C_s^{N+1}}{h}$	*Sink*	$\boldsymbol{SMI} = -\frac{\upsilon_t}{hSc}$

One can notice that when a term is a source of mass, then it is added explicitly while when it is a sink for concentration,

it is added implicitly. The fractional/variational resolution of the layer concentration evolution may induce mass creation or losses during the numerical solving. The final balance of mass must be verified over different tests cases and for different type of tracers.

III. VALIDATION METHODOLOGY

A. Test cases: hydrodynamic and forcing

The model mass conservation is assessed over three test cases based on two different meshes. The first two cases use an identical mesh and simply test the masses transfer over a basic rectangular flume with and without flow. For both cases, the initial free surface elevation is constant and fixed at $11m$. The flume width is of $80.89m$ while its length of $281.53m$. In the first scenario, all the boundaries are closed resulting in an immobile water tank. In the second scenario a constant flow, $Q = 50m^3/s$ and elevation $h = 11m$ are imposed upstream at $X = 0m$ and downstream at $X = 281.53m$ over a limited part of the lateral boundary. The upstream and downstream liquid boundaries do not cover the full lateral extent of the domain. That way, a non-uniform velocity field is created inside the domain.

A triangular mesh of 1100 nodes is used to discretize the domain. Figure 2 shows the velocity field in the flume for the second test case and after 2 hours. For these two scenarios we use a time step for the resolution of $15s$.

The third test case is here to assess how tidal flats will affect the mass transfer of the module. Thus, the focus is taken on a larger zone. The domain extends 15-km in x wise and 7-km y wise. The bottom elevation evolves linearly from $-50m$ at $X = 0$ to $+10m$ at $X = 15km$ while remaining constant in the y-direction. The triangular mesh discretizing the domain is made of ~12400 nodes of equal size around 100m. Initially, the water is immobile with a constant and null free surface elevation.

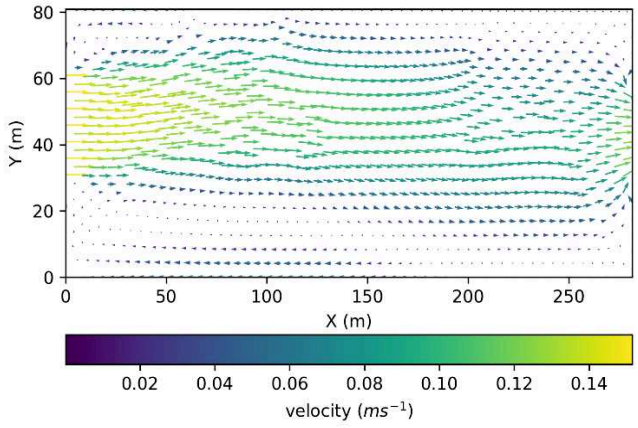

Figure 2. Second test case depth-averaged velocity after 2 hours of simulation. The bottom depth is homogenous and the free surface elevation remains constant at 11m. Initially, the water is still, a constant discharge of $50m^3s^{-1}$ forces the domain upstream (30≤Y≤60m) and downstream (35≤Y≤60m). All the boundaries are closed for the tracers.

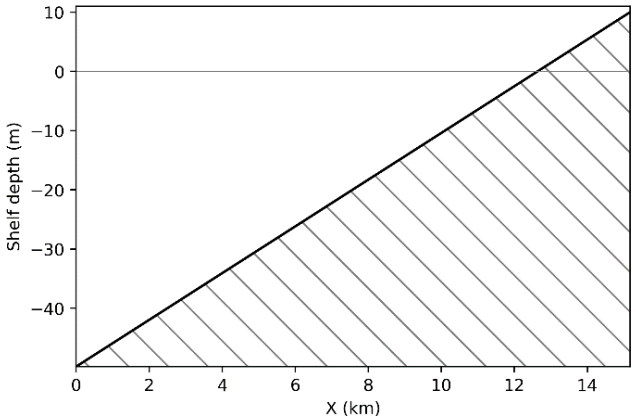

Figure 3. Longitudinal cross section of third test case with bathymetry. The left boundary represents the deep sea while the right one is the coastline. The depth goes linearly from -50m, at X=0m, to 10m at X=15km. The sea boundary is forced with a sea surface wave of amplitude 0.3m and period 12h. All the boundaries are closed for the tracers. The grey horizontal line is the initial water elevation.

The model is forced at $X = 0$ by a sinusoidal wave of amplitude 0.3m and period of 12 hours. This model, with its bathymetry and forcing is a schematization of a North Sea coastline under the main tidal component M2. For the three scenarios, the domain is always closed for tracer allowing easier comparison between initial and final mass. A constant turbulent viscosity for the surface and the suspended layer of $10^{-6}m^2/s$ is used. The bottom friction is characterized by a constant Chézy coefficient of $65m^{1/2}/s$.

While the wave equation solves the shallow water flow [16] [17], the classical resolution method is used for the tracer advection diffusion. For all the three scenarios, the bedload is made of a unique layer without cohesive sediments. Bedload transport is allowed following van Rijn's equation. Its validity range for particle size matches the size of particles generally sampled in the North Sea or its major influents. No erosion is permitted from the bottom thanks to the definition of a high critical shear stress.

B. Initial condition on tracers and buoyancy.

A unique class of plastic is inputted in the models. This class is defined as non-cohesive sediment and characterized by a constant absolute settling velocity of $|w_s| = 1.10^{-3}m/s$. For all three test cases, three scenarios are tested with varying initial conditions and buoyancy:

- Initial mass in the **surface layer** with **settling** plastic ($w_s > 0$). Surface plastics are expected to be transferred into suspension and then in the bedload.
- Initial mass in the **suspended layer**, with **settling** plastic ($w_s > 0$). Tracers will go directly into the bedload layer. Only a minimal fraction of the initial mass will go into the surface due to mixing. The rest of the exchanges follows what is already implemented in Telemac2D and Gaia.
- Initial mass in suspension, with **buoyant** plastic ($w_s < 0$). Plastic mass will go from suspension to the floating

layer with turbulent mixing dampening the buoyancy flux.

The simulations are run until vertical mass equilibrium is reached.

IV. RESULTS

A. Mass conservation

For the first two test cases and for all three scenarios, the model converges towards the expected and aforementioned behaviours. For test case 1 and for the three scenarios, the relative evolution of plastic mass in respect of time is represented in figure 4. The final mass creation or loss is shown in Table IV for the first two test cases.

For the first scenario, shown in Figure 4a, mass is transferred from the surface layer to the suspension and then reaches the bottom layer where it is kept. The total mass creation is equal to 0.136% for all scenarios where suspended and surface layer have exchanges. When comparing the time taken by the mass transfer with the time for a particle, with the given settling velocity w_s, to travel $11m$, Δt, (represented by the vertical grey line), one can notice that for scenario (a), at Δt maximal suspended mass is reached. Furthermore, the time needed by the simulation to reach full mass transfer to the bottom is approximatively twice Δt. This stems from the characteristic length chosen for the buoyant fluxes definition which is h for fluxes from floating to suspension and suspension towards bed.

This could be modified by assuming that floating particles travel a smaller vertical distance before reaching the suspension layer. In Figure 4b, the initial mass is set to the suspended layer and is totally transferred to the bedload. Figure 4c shows identical behaviour except that, as buoyant, the mass is transferred accordingly towards the surface. At Δt, around 60% of the initial mass have been transferred. Scenario (b) creates a negligible amount of mass as fluxes are mostly handled by Telemac2D and Gaia and can be taken as reference for the mass conservation of the module. The two vertical exchanges and their implementation introduces a mass creation of 0.1%. There is limited however not negligeable error in the mass conservation. One could wonder which of the exchange is responsible for this divergence.

Table IV Relative final mass for the test case 1 and 2. The mass are rounded up to three decimals.

	Mass lost / created (%)	
Scenario / test cases	**Test case 1**	**Test case 2**
(a)	0,136	0,136
(b)	$\mathbf{1.5\ 10^{-5}}$	$\mathbf{9.4\ 10^{-4}}$
(c)	0,136	0,136

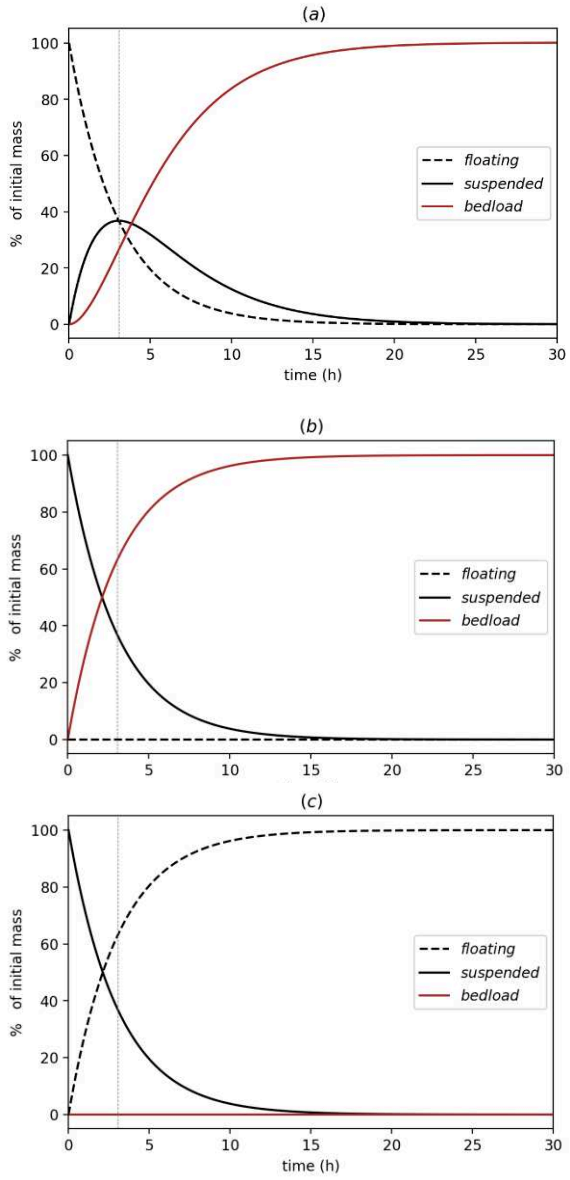

Figure 4. Relative mass evolution of the three layers in test case 1 for scenarios (a), (b) and (c) in vertical order. The vertical grey line at $t = \Delta t \sim 3h$ represents the time for a particle, with the given settling velocity, to travel the water depth of 11m.

B. Implicitation for vertical mixing fluxes

To identify the source of the created mass, the buoyant or the mixing flux, additional calculations were performed with changes in the fluxe implementation. Three configurations were observed. The first one is the implicit-explicit expression of the buoyant and mixing fluxes, seen in Table II and III. The second configuration removes the mixing fluxes while the last one considers an only explicit implementation for the turbulent fluxes. Table V summarizes the results on mass creation.

Table V Table V Relative final mass for different implementation of the vertical fluxes for test case 1 and 2

Flume	Test case:	1	2		
	Mixing fluxes implementation:	*Implicit explicit*	*none*	*explicit*	*Implicit explicit*
Mass difference (%)	*(a)*	0.136	0.136	0.136	0.136
	(b)	$\mathbf{1.6\ 10^{-5}}$	$\mathbf{1.0\ 10^{-3}}$	$\mathbf{1.0\ 10^{-3}}$	$\mathbf{1.0\ 10^{-3}}$
	(c)	0.136	$\mathbf{4.10^{-3}}$	0.136	0.136

No significant changes were observed when using an explicit implementation of the vertical mixing fluxes. For scenario (a), mixing has limited influence since mass is rather quickly transferred towards the suspension and then the bottom. In the other hand, in scenario (c), the mixing exchanges are more significant since the mass settles in the surface layer with continuous mixing with the suspension. For all configurations with mixing fluxes, the mass creation is of the same order. However, when there is no mixing and for scenario (c) mass creation drops significantly to reach the level of mass created in scenario (b). The combined turbulent and buoyant fluxes induce limited mass creation. Thereafter, the implicit-explicit implementation will be kept as providing more stability to the equations especially over tidal flats.

C. *Tidal flats*

Over test case 3 and for scenarios (a), (b) and (c) the model's advection diffusion equation does not converge anymore due to the inter tidal area located between kilometres 12 and 13 of the schematized shelf. However, functioning over tidal flats is crucial for the intended use of the final process-based model. Thus, to overcome this divergence, two solutions artificially removing the dry elements from the calculation of the vertical fluxes were investigated.

The first one, α, keeps the same implementation as before. It uses the NERD scheme for the resolution of the advection of tracers with free surface gradient correction and a minimum threshold, $h_{\lim}$, on the free surface elevation to define the mixing and buoyant fluxes. Several different limit values were tested and their respective results in term of convergence and final mass conservation are shown in table VI.

The second option, named β, is to use masking of the dry elements along with the LIPS scheme for the advection. Mass conservation of this method is shown in the same table. In both cases, the explored solution is not ideal as adding sharp limits, such as clipping on the elevation, results in the creation or removal of mass. For configuration α, the model was converging only when $h_{\lim} > 0$. Full explicit implementation of the mixing fluxes did not allow convergence of the model in neither of the tidal flat configuration. Here again, there is limited mass creation for scenario (b) and all configuration, due to the limited exchanges between the surface and the suspended layers. However, for the other scenarios, the created/lost mass in not negligible anymore and reaches the order of one percent to divergence, especially when the elevation threshold becomes too low for configuration (c). Configuration α with a high enough threshold (0.1m) seems to limit mass creation for all scenarios. Configuration β does not allow convergence for (a) and (c). The issues that arise with tidal flats are challenging and requires further in-depth study.

D. *Implicitation for tracers concentration*

Another lead was explored to reduce the mass creation in cases with and without tidal flats: eventual implication of the concentrations in the fractional resolution of the concertation at a given time step. Once step 4 of the resolution is reached (Table VI), instead of using the newly obtained suspended concentration to calculate the explicit fluxes of the surface layer an implication on C_s^N and C_s^{N+1} is used with a factor θ. Thus, the used concentration is T, obtained from (8).

Table VI Table VI Final mass creation / losses on the third test case with tidal flats and for the two different implementations. Different thresholds were tested for the first configuration α

Test case 3		α			β
$h_{\lim}$ (m)		0.1	0.05	0.01	
Mass difference (%)	*(a)*	-0.949	-0.592	8.231	120.259
	(b)	-0.097	-0.097	-0.096	-0.100
	(c)	0.833	1.666	1.24e18	diverge

$$C_s = \theta C_s^N + (1-\theta) C_s^{N+1} \quad (8)$$

This configuration was tested for different values of the implication factor ($0 \leq \theta \leq 1$) and for test case (c). Indeed, for this test case, the tracer class is buoyant linked with an explicit expression of the buoyant flux.

Furthermore, due to the fractional resolution method, the surface tracer concentration at time N is not kept in memory when calculating the floating concentration at time N+1. For test case 3, the results are based on tidal flat configuration α with a limit threshold of 0.1m. Table VII present the results for different implication factors. There is significant improvement when the implication factor is null for test case (2) without tidal flats while limited progress for the test case (3). When C_s^N, suspended concentration of the last time step, is used to calculate the source and sink terms for the surface layer.

Table VII Implication of suspended concentration influence on final mass

Test case – configuration (c)	Mass created / lost (%)		
	$\theta = 1$	$\theta = 0.5$	$\theta = 0$
2-Flume	0.136	0.068	0.003
3-Coast	0.833	0.769	0.731

V. CONCLUSION

A newly developed three-layer module for TELEMAC-2D and GAIA, for a full process-based model for riverine plastic fluxes has been developed and tested for simple schematized cases.

The proposed numerical implementation of an additional surface layer and the implied vertical fluxes results in limited mass creation in a simple flume without tidal flats for both buoyant and settling plastic classes. For tidal flats, convergence is guaranteed only when imposing a strict limit on the free surface elevation for the vertical fluxes to exist. This strict limit generates significant mass creation that may be containable with manual optimization of the threshold or other implementations. Tidal flats consideration appears rather challenging but are crucial for the intended use of the full model (i.e. dealing with beached plastics) and the author hope that future work on that topic may help to improve the results.

The next step to be investigated and implemented are the different processes affecting riverine plastic (i.e. fragmentation, erosion, biofouling and sediment interaction) for each of them, theoretical or empirical laws must be deduced based on literature, observations or experiments and implemented inside the module. Then drift from external parameters such as wind or waves could also be added as a correction of the surface velocity. Finally, as the control of the presented module is (for now) hard coded using Fortran files, the user friendliness of the module would be considerably improved by the reading of a steering file for monitoring plastics in the simulation.

ACKNOWLEDGEMENT

This work is carried out in the framework of the EU H2020 LABPLAS project (www.LABPLAS.eu) and the Flemish SBR PLUXIN project funded through VLAIO and the Flemish Blue Cluster (www.PLUXIN.be).

REFERENCES

[1] Law, K. L. (2017). Plastics in the Marine Environment. *Annual review of marine science*, *9*, 205-229.

[2] Schmidt, C., Krauth, T., & Wagner, S. (2017). Export of plastic debris by rivers into the sea. *Environmental science & technology*, *51*(21), 12246-12253.

[3] Schöneich-Argent, R. I., Dau, K., & Freund, H. (2020). Wasting the North Sea?–A field-based assessment of anthropogenic macrolitter loads and emission rates of three German tributaries. *Environmental Pollution*, *263*, 114367.

[4] Kooi, M., Reisser, J., Slat, B., Ferrari, F. F., Schmid, M. S., Cunsolo, S., Brambini, R., Noble, K., Linders, T.E.W., Schoeneich-Argent, R. & Koelmans, A. A. (2016). The effect of particle properties on the depth profile of buoyant plastics in the ocean. *Scientific reports*, *6*(1), 1-10.

[5] Reisser, J., Slat, B., Noble, K., Du Plessis, K., Epp, M., Proietti, M., ... & Pattiaratchi, C. (2015). The vertical distribution of buoyant plastics at sea: an observational study in the North Atlantic Gyre. *Biogeosciences*, *12*(4), 1249-1256.

[6] Waldschläger, K., & Schüttrumpf, H. (2019). Effects of particle properties on the settling and rise velocities of microplastics in freshwater under laboratory conditions. *Environmental science & technology*, *53*(4), 1958-1966.

[7] Fischer, R., Lobelle, D., Kooi, M., Koelmans, A., Onink, V., Laufkötter, C., ... & van Sebille, E. (2022). Modeling submerged biofouled microplastics and their vertical trajectories. *Biogeosciences Discussions*.

[8] Jahnke, A., Arp, H. P. H., Escher, B. I., Gewert, B., Gorokhova, E., Kühnel, D., ... & MacLeod, M. (2017). Reducing uncertainty and confronting ignorance about the possible impacts of weathering plastic in the marine environment. *Environmental Science & Technology Letters*, *4*(3), 85-90.

[9] Kukulka, T., Proskurowski, G., Morét-Ferguson, S., Meyer, D. W., & Law, K. L. (2012). The effect of wind mixing on the vertical distribution of buoyant plastic debris. *Geophysical Research Letters*, *39*(7).

[10] Andersen, T.J., Rominikan, S., Olsen, I.S., Skinnebach, K.H., Fruergaard, M., 2021. Flocculation of PVC microplastic and fine-grained cohesive sediment at environmentally realistic concentrations. *Biological Bulletin* 240, DOI:10.1086/712929.

[11] Scherer C, Weber A, Stock F, Vurusic S, Egerci H, Kochleus C, Arendt N, Foeldi C, Dierkes G, Wagner M, Brennholt N, Reifferscheid G. (2020) Comparative assessment of microplastics in water and sediment of a large European river. Sci Total Environ. 2020 Oct 10;738:139866. doi: 10.1016/j.scitotenv.2020.139866.

[12] Audouin, Y., Benson, T., Delinares, M., Fontaine, J., Glander, B., Huybrechts, N., ... & Walther, R. (2019). Introducing GAIA, the brand new sediment transport module of the TELEMAC-MASCARET system. In *XXVIth TELEMAC-MASCARET User Conference, 15th to 17th October 2019, Toulouse*.

[13] Domercq, P., Praetorius, A., & MacLeod, M. (2022). The Full Multi: An open-source framework for modelling the transport and fate of nano-and microplastics in aquatic systems. *Environmental Modelling & Software*, *148*, 105291.

[14] Toorman, E.A. (2008). Vertical mixing in the fully developed turbulent layer of sedi- ment-laden open-channel flow. J. Hydraul. Eng. 134 (9), 1225–1235 .

[15] Toorman, E.A. (2009). Errata and addendum for “Vertical mixing in the fully devel- oped turbulent layer of sediment-laden open-channel flow”by EA Toorman. J. Hydraul. Eng. 135 (6), 538 -538

[16] Hervouet, J. M., & Razafindrakoto, E. (2005). The wave equation applied to the solution of Navier-Stokes equations in finite elements. *WIT Transactions on the Built Environment*, *78*.

[17] Hervouet, J. M. (2007). *Hydrodynamics of free surface flows: modelling with the finite element method*. John Wiley & Sons.